WORLD CONFERENCE ON TIMBER ENGINEERING 2025
BRISBANE, AUSTRALIA
Advancing Timber for the Future Built Environment

EFFECT OF NAIL JOINT STIFFNESS ON THE IN-PLANE SHEAR AND OUT-OF-PLANE BENDING PROPERTIES OF NLT

Kazuki Ito[1], Shiro Nakajima[2]

ABSTRACT: Nail laminated timber (NLT) is composed of sawn boards connected by nail joints. To develop design methods for NLT based on the stiffness of the nail joints NLT composed of steel or aluminum nails, which have different stiffness, were produced and tested for their in-plane shear properties. The shear strength and initial stiffness of NLT with aluminum nails were 60-65% of those with steel nails. NLT was modeled to verify the ratio of embedment work out of the total work that is the summation work caused by the shear deformation of nail joints between laminations, embedment of lumber into the mudsill and beam, and bearing pressure and friction between laminations. NLT with higher-stiffness nail joints showed a higher rate of embedment work compared to that with lower-stiffness nail joints. NLTs were also tested for out-of-plane bending. The bending modulus of elasticity and strength of NLTs composed of aluminum nails were nearly equivalent to those composed of steel nails. NLT was also modeled to verify the ratio of bending deformation and rotational deformation of butt jointed lumbers. Lumbers joined by lower-stiffness nails showed a higher rate of rotational deformation than those joined by higher-stiffness nails.

KEYWORDS: Nail Laminated Timber, In-plane shear, Out-of-plane bending, aluminum nails, butt joint

1 INTRODUCTION

Nail Laminated Timber (NLT) is composed of sawn boards and joined with nails. Therefore, the structural properties of NLT are governed by the stiffness of the nail joints. Structural guidelines for NLT [1][2] provide methods for evaluating the design values of NLT. However, there seems to be no description of how to consider the stiffness of nail joints in the evaluation process. This paper focuses on the design methods for NLT for their in-plane shear and out-of-plane bending properties and presents methods for calculating these properties while considering the stiffness of nail joints. The NLT specimens were fabricated using steel and aluminum nails, which have different stiffnesses. In-plane shear and out-of-plane bending tests were conducted. Furthermore, the load-deformation curves were calculated and compared with the test results.

2 NAILS USED FOR NLTs

2.1 NAIL TYPES AND SIZES

Table 1 presents the nail types and sizes used for NLT specimens.

***Table 1**: Nail types and sizes*

Nail types	Diameter (mm)	Length (mm)
Steel	3.76	75
Aluminum	5.00	77

2.2 NAIL JOINTS TEST

Test specimens

Figure 1 illustrates the test specimens. The test specimens were made of Japanese Cedar (Cryptomeria japonica) with an average MOE of 10.4GPa. Two types of loading conditions were applied: perpendicular and parallel to the grain. The nail joints were made using steel nails and aluminum nails as listed in Table 1. For each steel nail and aluminum nail specimen, three specimens were fabricated for each loading direction.

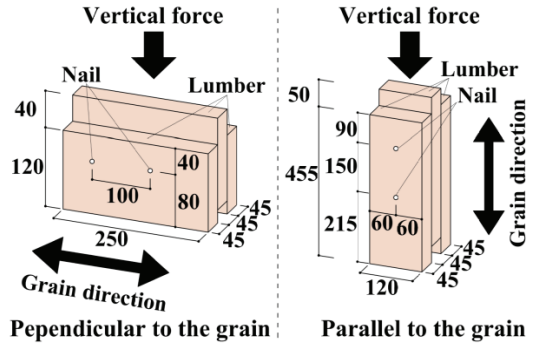

***Figure 1:** test specimens of nail joints test*

Testing method

For the four types of specimens, a vertical load was applied to the central piece of the three laminated lumber members in the specimen, and the ultimate load was obtained (see Figure 1). Then, the remaining two

[1] Kazuki Ito, Utsunomiya University, Japan, mc246226@s.utsunomiya-u.ac.jp

[2] Shiro Nakajima, Utsunomiya University, Japan, s-nakajima@cc.utsunomiya-u.ac.jp

https://doi.org/10.52202/080513-0273

members of each specimen were subjected to one-way cyclic loading. This one-way cyclic load was applied at the vertical deformation corresponding to 1.25%, 2.5%, 5%, 7.5%, 10%, 20%, 40%, 60%, 80%, and 100% of the ultimate deformation.

Test results

The envelopes of the load-deformation curves are shown in Figure 2 and characteristic values are shown in Table 2.

The yield shear strength of the nail joint perpendicular to the grain is almost equal to the parallel. The yield shear strength of aluminum nails was equal to that of steel nails. The initial stiffnesse of aluminum nail joints was almost 70% of that of steel nail joints.

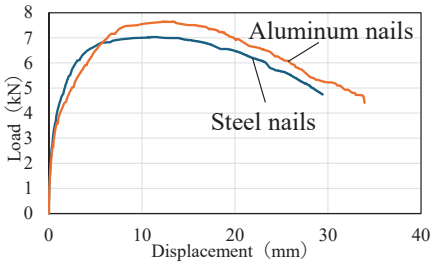

(a) Parallel to the grain

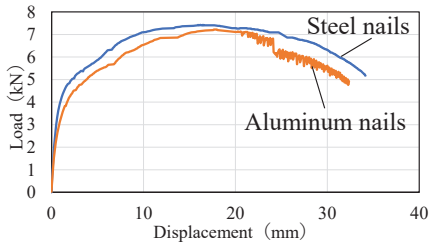

(b) Perpendicular to the grain

***Figure 2**: Load-displacement relationships for the nail joints*

***Table 2**: Characteristic values of the nail joints*

Nail types	Characteristic Values			
	Perpendicular to the grain		Prallel to the grain	
	Yield shear strength *Py* (kN)	Initial stiffness *K* (kN/mm)	Yield shear strength *Py* (kN)	Initial stiffness *K* (kN/mm)
Steel	0.99	3.72	0.95	4.56
Aluminum	1.04 (104%)	2.57 (69%)	0.93 (98%)	3.22 (71%)

Note: the values in ( ) represent the ratio relative to the steel nail joints

3 IN-PLANE SHEAR PROPERTY

3.1 EXPERIMENTAL INVESTIGATION

Test specimen

The test specimen is shown in Figure 3. The lumber species is Japanese Cedar (Cryptomeria japonica) with an average MOE of 9.35GPa and an average density of 368kg/m^3. Each specimen consists of 20 laminations (sawn boards), each measuring 1900mm in length, 120mm in width, and 45mm in thickness, joined using steel and aluminum nails (see Table 1).

The interval between adjacent nail joints along the length of the lumber is 200mm, with two rows of nails. The nail joints between adjoining laminations are shifted by 100mm to prevent overlap. The distance from the nail joint to the edge of the lumber is 25mm.

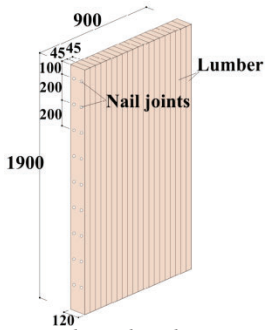

***Figure 3:** test specimen under in-plane shear*

Testing method

The setup for the shear test is shown in Figure 4. The specimens are fixed to the frame consisting of a Mudsill (120mm in width and height), beam (120mm in width and 240mm in height), and columns (120mm in width and height). The left and right ends of the beam were connected to the base frame of the testing equipment by tiedown rods.

Reverse cyclic loads were applied to the top of the test specimens. Three repetitive reverse cyclic loads were applied at the shear deformation level of approximately 1.67×10^{-3} (1/600) rad, 2.22×10^{-3} (1/450) rad, 3.33×10^{-3} (1/300) rad, 5.00×10^{-3} (1/200) rad, 6.67×10^{-3} (1/150) rad, 8.33×10^{-3} (1/120) rad, 10.0×10^{-3} (1/100) rad, 13.3×10^{-3} (1/75) rad, 20.0×10^{-3} (1/50) rad, and after this cyclic loading the test specimens were loaded to the shear deformation level 83.3×10^{-3} (1/12) rad.

The horizontal displacement at the top and bottom of the test specimens, the vertical displacement at both the left and right bottom of the test specimens, and the relative displacement between the laminations were measured.

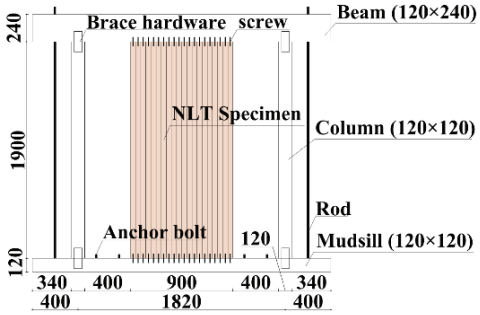

***Figure 4**: Setup of the shear test*

Test results

The positive envelopes of the load-deformation angle curves are presented and compared for NLT with steel and aluminum nails in Figure 5. The horizontal axis represents the true shear deformation angle and the method for calculating this angle is shown in Figure 6. The vertical dashed lines in Figure 5 indicate the true deformation angles of 1/150rad and 1/15rad. The load corresponding to each displacement is considered either the yield load (*Py*) or the maximum load (P_{max}). The in-plane shear capacity is defined as the yield load (*Py*). The initial stiffness is defined as the slope of the line connecting the yield load (*Py*) and the origin. The shear capacity (*Py*) and

https://doi.org/10.52202/080513-0273

initial stiffness (K) for each NLT specimen are given in Table 3. The initial stiffness of the NLT with aluminum nails was 63% of that with steel nails. The in-plane shear capacity of NLT with aluminum nails was 65% of that with steel nails.

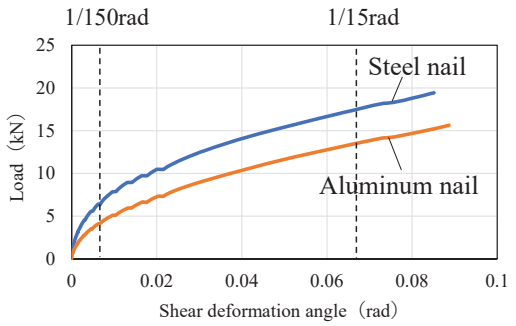

Figure 5: *Positive envelopes of the load deformation curves*

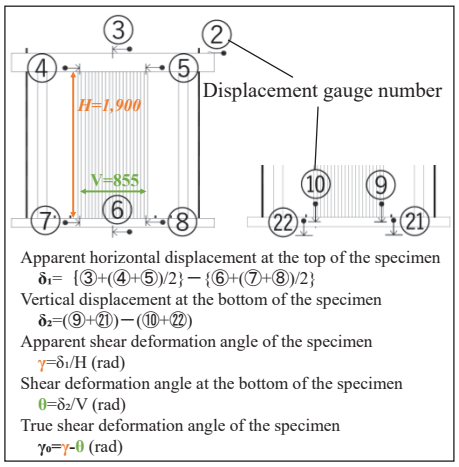

Figure 6*: method for calculation the ture shear deformation angle*

Table 3*: Characteristic values of the NLTs*

Nail types	Characteristic Values	
	Initial stiffness K (kN/mm)	Shear capacity Py (kN)
Steel	0.52	6.34
Aluminum	0.33 (63%)	4.13 (65%)

Note: the values in () represent the ratio relative to steel nail joints.

3.2 CALCULATION OF LOAD-DISPLACEMENT RELATIONSHIP

Calculation method

The deformation of the NLT applied to in-plane shear force can be modeled as shown in Figure 7.
When the NLT panel has a shear deformation angle θ(rad), the deformation at the top of the NLT panel δ_{NLT} can be calculated by (1).

$$\delta_{NLT} = \theta \cdot H \tag{1}$$

Where H is the height of the NLT specimen.
When the shear deformation angle is θ(rad), the shear deformation of the nails ($\delta_{nail}(\theta)$) can be calculated by (2).

$$\delta_{nail}(\theta) = b \cdot \sin\theta \tag{2}$$

Where b is the width of the lamination.
The load ($F_{nail}\{\delta_{nail}(\theta)\}$ - displacement ($\delta_{nail}(\theta)$) relationships at the nail joints were derived from the test results of the joints under parallel to the grain loading (see Figure 2(a)).
The internal energy consumption ($E_{INT\text{-}nail}(\theta)$) caused by shear deformation at the nail joints can be calculated as (3).

$$E_{INT\text{-}nail}(\theta) = s\times \int_{\theta 1}^{\theta 2} F_{nail}\{\delta_{nail}(\theta)\} \cdot \delta_{nail}(\theta) d\theta \tag{3}$$

Where s is the number of nail joints ($s=m\times(n-1)$), m is the number of nail joints per layer between laminations, and n is the number of laminations.

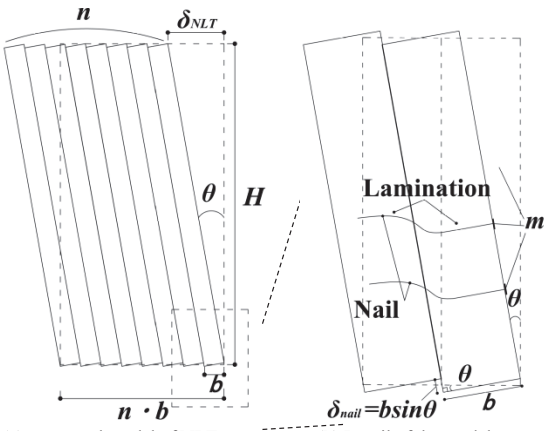

(a) Structural model of NLT **(b)** Detail of the model

Figure 7: *Structural modeling of NLT applied to in-plane shear force*

When the shear deformation of NLT increases, the ends of the laminations embed in the beam and mudsill, as showan in Figure 8.
When the NLT panel has a shear deformation angle θ(rad), the embedment force ($F_{emb}(\theta)$) can be calculated by (4).

$$F_{emb}(\theta) = \frac{x^2 y_0 E_{90}\theta}{z}\left\{\frac{1}{2}+\frac{2z}{3x}\left(1-e^{-\frac{3x_1}{2z}}\right)\right\} \tag{4}$$

Where x is the distance from the tip of the embedment to the center of rotation of the end of the lamination, x_1 is the lamination thickness (45mm), y_0 is the lamination width (120mm), z is the height of the beam or mudsill (120mm), and E_{90} is the modulus of elasticity for full compression at perpendicular to the grain (0.28GPa).
The internal energy consumption ($E_{INT\text{-}emb}(\theta)$) caused by embedment at the bottom or top of the lamination into the beam or mudsill can be calculated as (5).

$$E_{INT\text{-}emb}(\theta) = 2n\times \int_{\theta 1}^{\theta 2} F_{emb}(\theta) \cdot \frac{2}{3} x\theta d\theta \tag{5}$$

When the shear deformation of NLT increases, the gap between the laminations adjoining each other decreases. As a result, the bearing stress on the wide side face of the lamination due to embedment will occur (see Figure 9).

https://doi.org/10.52202/080513-0273

The stress derived by the embedment will increase as the shear deformation increases.
When the NLT panel has a shear deformation angle θ(rad), the depth of embedment of the lamination $\delta_{bear}(\theta)$ can be calculated as (6).

$$\delta_{bear}(\theta) = b(1-\cos\theta) \quad (6)$$

The load ($F_{bear}\{\delta_{bear}(\theta)\}$) - displacement ($\delta_{bear}(\theta)$) relationships between laminations were derived from the test results of full compression at perpendicular to the grain (see Figure 10).
The internal energy consumption ($E_{INT\text{-}bear}(\theta)$) caused by embedment between the laminations can be calculated as (7).

$$E_{INT\text{-}bear}(\theta) = (n-1) \cdot e \cdot A \cdot \int_{\theta 1}^{\theta 2} F_{bear}\{\delta_{bear}(\theta)\} \cdot \delta_{bear}(\theta) d\theta \quad (7)$$

Where $(n-1)$ is a number of gaps between the laminations, e is the reduction factor of contact area between the laminations, and A is the contact cross-section.
When the NLT panel undergoes shear deformation, friction stress will occur on the wide side face of the lamination.
When the NLT panel has a shear deformation angle θ(rad), the length of friction surface displacement between laminations ($\delta_{fric}(\theta)$)) can be calculated as (8).

$$\delta_{fric}(\theta) = b \cdot \sin\theta \quad (8)$$

The fiction stress ($F_{fric}\{\delta_{fric}(\theta)\}$) caused by bearing stress on the wide side of the lamination can be calculated as (9).

$$F_{fric}\{\delta_{fric}(\theta)\} = \mu \cdot F_{bear}\{\delta_{bear}(\theta)\} \quad (9)$$

Where μ is the coefficient of friction (0.3 in this study).
The internal energy consumption ($E_{INT\text{-}fric}(\theta)$) caused by friction between the laminations can be calculated as (10).

$$E_{INT\text{-}fric}(\theta) = (n-1) \cdot e \cdot A \cdot \int_{\theta 1}^{\theta 2} F_{fric}\{\delta_{fric}(\theta)\} \cdot \delta_{fric}(\theta) d\theta \quad (10)$$

The external energy consumption ($E_{EXT}(\theta)$) caused by the shear deformation θ(rad) of the NLT panel can be calculated as (11).

$$E_{EXT}(\theta) = \int_{\theta 1}^{\theta 2} P(\theta \cdot H) \cdot (\theta \cdot H) d\theta \quad (11)$$

Where P is the load applied at the top of the NLT panel.
The $E_{INT\text{-}total}(\theta)$ is equal to the $E_{EXT}(\theta)$ as shown in (12).
The load necessary to apply at the top of the NLT panel to give a certain deformation at the top of the NLT panel can be calculated.

$$E_{EXT}(\theta) = E_{INT\text{-}nail}(\theta) + E_{INT\text{-}emb}(\theta) + E_{INT\text{-}bear}(\theta) + E_{INT\text{-}fric}(\theta) \quad (12)$$

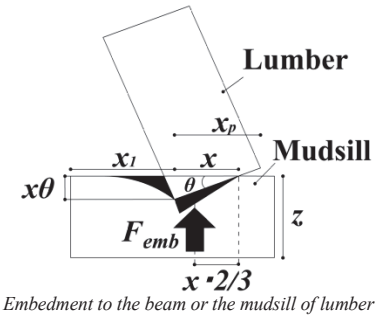

Figure 8: *Embedment to the beam or the mudsill of lumber*

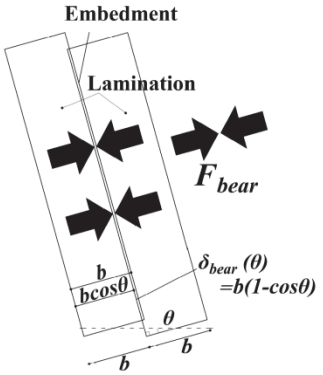

Figure 9: *Conceptual diagram of embedment between the laminations*

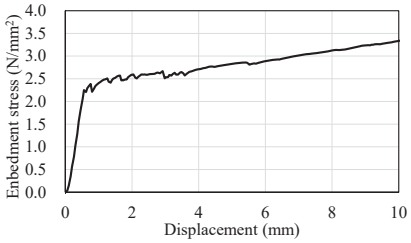

Figure 10*: Load-displacement relationships for full compression at perpendicular to the grain*

By conducting an incremental displacement analysis, the load-deformation curve of the NLT panels was estimated

Results of calculation

The results of the calculation are presented in Figures 11 and 12, compared with the test results. The red load-deformation angle curves in Figures 11 and 12 represent the test results. The black double lines of load-deformation angle curves in Figures 11 and 12 show the calculation results obtained by considering only the shear deformation of nail joints as internal energy consumption. These calculation results underestimated the load compared to the test results.
The black dashed lines in Figure 11 represent the load-deformation angle curves obtained by considering not only the shear deformation of nail joints but also the bearing compression and the friction between the laminations. These curves represent the results of calculating load-deformation angle curves with varying values of the reduction factors (e) for the contact area of the laminations.
Similarly, the black dashed lines in Figure 12 represent the load-deformation angle curves calculated by incorporating the same considerations as in Figure 11,

https://doi.org/10.52202/080513-0273

with the reduction factors (e) that best matched the test results. Additionally, these curves account for the embedment at the bottom or top of the laminations into the beam or mudsill as internal energy consumption, representing varying values of the distance (x) from the tip of the embedment to the center of rotation at the end of the laminations.

When comparing the results of the calculation with the test results, the impact of embedment at the bottom or top of the laminations into the beam or mudsill is significant up to approximately 0.03 (1/30) rad, after which the effects of bearing compression and friction between the laminations become more prominent. The reduction factors (e) that best matched the test results were approximately 0.4 for steel nails and 0.2 for aluminum nails. The NLT with steel nails shows a higher rate of embedment work against the total work than the NLT with aluminum nails (see Figures 11 and 12).

4 OUT-OF-PLANE BENDING PROPERTY

4.1 EXPERIMENTAL INVESTIGATION

Test specimens

The test specimens for the out-of-plane bending test are shown in Figure 13. The lumber species used is Japanese Cedar (Cryptomeria japonica), with the modulus of elasticity (MOE) provided in Table 4. Each specimen consists of 5 layers, measuring 6200mm in length, 225mm in width, and 120mm in thickness, joined with steel and aluminum nails (see Table 1). The specimens are labeled as [Steel nail-1], [Steel nail-2], [Aluminum nail-1], [Aluminum nail-2].

The nail joining methods for the out-of-plane bending test were the same as those used for the in-plane shear test.

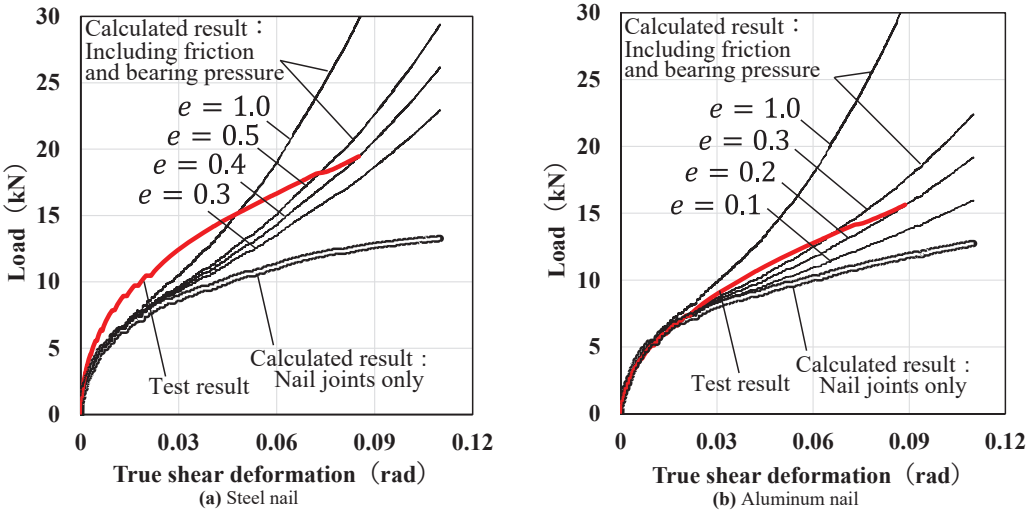

(a) Steel nail **(b)** Aluminum nail

***Figure 11**: Load-deformation curves: Comparison of experimental and calculated results (considering bearing pressure and friction between lumbers).*

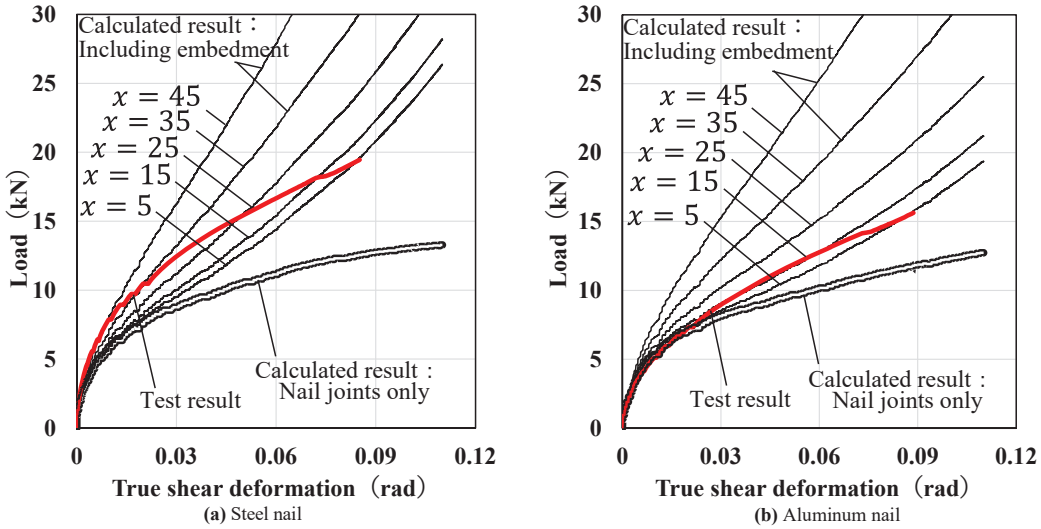

(a) Steel nail **(b)** Aluminum nail

***Figure 12**: Load-deformation curves: Comparison of experimental and calculated results (considering bearing pressure, friction between lumbers, and embedment to the beam or the mudsill of lumbers).*

https://doi.org/10.52202/080513-0273

The butt-joint area was reinforced by adding additional nail joints 30mm from the butt joint on both sides.

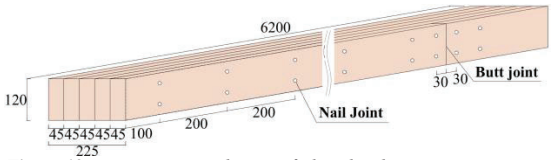

***Figure 13**: test specimen under out-of-plane bending*

***Table 4**: Average modulus of elasticity of each specimen*

Specimen name	Modulus of elasticity (GPa)
Steel nail-1	9.89
Steel nail-2	9.6
Aluminum nail-1	9.61
Aluminum nail-2	10.15

Testing method

The setup for the bending test is shown in Figure 14. The span of the NLT specimen was 6000mm and a four-point bending test was conducted until the specimens failed. Vertical displacements at both support points and at the center of the NLT specimen were measured.

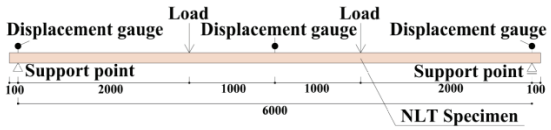

***Figure 14**: Setup of the out-of-plane bending test*

Test results

The load-deformation curves for the out-of-plane bending test are presented in Figure 15, and the modulus of elasticity in bending and bending strength are shown in Table 5. The load was linearly increased until the maximum load for each specimen, after which it rapidly declined. The bending modulus of elasticity and strength of NLTs with aluminum nails were almost equivalent to those with steel nails, and the MOE ratios of the lumber consisting of each NLT were assumed to be almost the same.

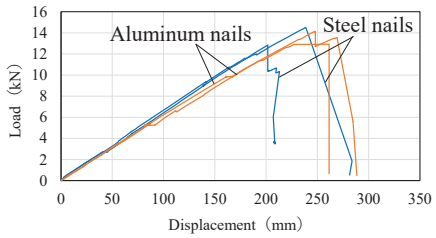

***Figure 15:** Load deformation curves for the out-of-plane bending test*

***Table 5**: Characteristic values of the NLTs*

Nail types	Characteristic Values	
	Modulus of elasticity in bending E(kN/mm^2)	Bending strength σ_{max} (N/mm^2)
Steel	7.57	25.33
Aluminum	7.32 (97%)	25.05 (99%)

Note: the values in () represent the ratio relative to steel nail joints.

4.2 CALCULATION OF LOAD-DISPLACEMENT RELATIONSHIP

Calculation method

The load-deformation curves of NLT were calculated by considering the shear deformation of nail joints, the bending deformation of lumbers, and the rotational deformation of lumbers with a butt joint between the force points, using incremental analysis.

The vertical displacement at the center of the span was defined as δ(mm), while that at the load points was defined as δ_1(mm), as shown in Figure 16.

When the displacement at the load points is δ_1, the load applied to the NLT specimen was defined as $F_{NLT}(\delta 1)$.

The external energy consumption $E_{EXT}(\delta_1 \rightarrow \delta_1+\Delta\delta_1)$ caused by the bending deformation from δ_1 to $\delta_1+\Delta\delta_1$ at the load points of the NLT panel can be calculated as (13).

$$E_{EXT}(\delta_1 \rightarrow \delta_1+\Delta\delta_1) = \frac{1}{2}\{F_{NLT}(\delta_1) + F_{NLT}(\delta_1 + \Delta\delta_1)\} \times \Delta\delta_1 \quad (13)$$

The internal energy consumption in NLT panels consists of the bending deformation of the lumbers and the shear deformation of nail joints. Lumbers without butt joints between the load points were assumed to undergo only bending deformation. In contrast, lumbers with butt joints between the load points were assumed to undergo both bending deformation and rotational deformation with the support points serving as the center of rotation. The difference in deformation between lumbers with butt joints and those without butt joints between the load points corresponds to the shear deformation in the nail joints. This shear deformation causes the internal energy consumption of the nail joints.

When the displacement at the load points changes from δ_1 to $\delta_1+\Delta\delta_1$, the internal energy consumption ($E_{INT\text{-}beam}(\delta_1 \rightarrow \delta_1+\Delta\delta_1)$) caused by only bending deformation of two out of five lumbers without butt joints between the load points can be calculated as (14).

$$E_{INT\text{-}beam}(\delta_1 \rightarrow \delta_1 + \Delta\delta_1) = \frac{1}{2}\left\{\frac{2}{5}F_{NLT}(\delta_1)+\frac{2}{5}F_{NLT}(\delta_1+\Delta\delta_1)\right\} \times \Delta\delta_1 \quad (14)$$

When vertical loads are applied to the NLTs, the greatest deformation occurs at the center of the span, while no deformation occurs at the support points. A relationship of δ_1 and δ is given as (15).

$$\delta_1 = \frac{20}{23}\delta \quad (15)$$

The difference in vertical displacement of nail joints between lumbers without butt joints and those with butt joints between the load points represents the amount of shear deformation of nail joints.

When the displacement at the load points is δ_1, the shear deformation ($\delta_{nail(x)}(\delta)$) of nail joints is given as (16) and (17) using the reduction factor n explained later. The shear deformation ($\delta_{nail(x)}(\delta)$) is distinguished between two cases ((16), (17)) and for $4000 \leqq x \leqq 6000$, it is assumed to follow (16) due to symmetrical bending behavior.

https://doi.org/10.52202/080513-0273

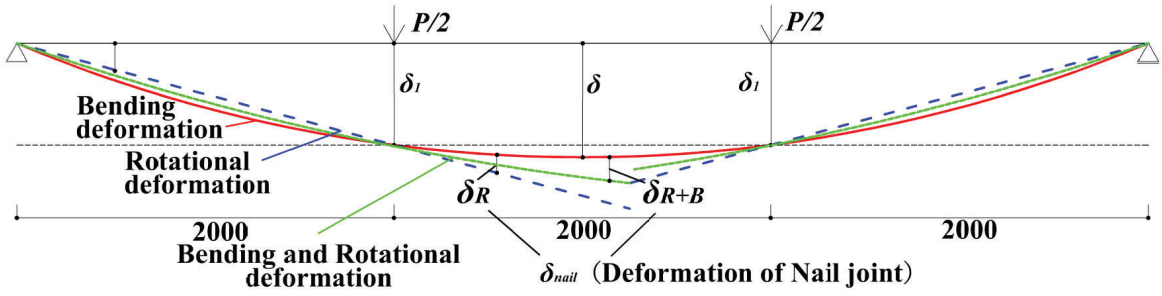

***Figure 16**: Structual model for out-of-plane bending*

$$(0 \le x \le 2000)$$
$$\begin{aligned}\delta_{nail(x)}(\delta) &= n \cdot \{\delta_{B(x)}(\delta) - \delta_{R(x)}(\delta)\} \\ &= n \cdot \left\{\frac{24x\delta}{23 \cdot 2000^3}\left(-\frac{x^2}{6}+2000^2\right) - \frac{x\delta}{2300}\right\} \\ &= n \cdot \frac{x\delta}{23}\left(-\frac{4}{2000^3}x^2+\frac{1}{500}\right) \end{aligned} \quad (16)$$

$$(2000 \le x \le 4000)$$
$$\begin{aligned}\delta_{nail(x)}(\delta) &= n \cdot \{\delta_{R(x)}(\delta) - \delta_{B(x)}(\delta)\} \\ &= n \cdot \left\{\frac{x\delta}{2300} - \frac{\delta}{2300 \cdot 10^4}(-3x^2+18000x - 2000^2)\right\} \\ &= n \cdot \frac{\delta}{2300}\left(\frac{3}{10000}x^2 - 0.8x+400\right) \end{aligned} \quad (17)$$

Where x is the distance from the support point and $\delta_{B(x)}(\delta)$ represents the vertical displacement caused by only bending of the lumber at a distance x from the support point. $\delta_{B(x)}(\delta)$ is given by (18) and (19).

$$(0 \le x \le 2000)$$
$$\delta_{B(x)}(\delta) = \frac{24x \cdot \delta}{23 \cdot 2000^3}\left(-\frac{x^2}{6}+2000^2\right) \quad (18)$$

$$(2000 \le x \le 4000)$$
$$\delta_{B(x)}(\delta) = \frac{\delta}{2300 \cdot 10^4}\left(-3x^2+18000x - 2000^2\right) \quad (19)$$

$\delta_{R(x)}(\delta)$ represents the vertical displacement at a distance x from the support point, caused only by rotation with the support points serving as the center of rotation for the lumber. $\delta_{R(x)}(\delta)$ is given by (20).

$$\delta_{R(x)}(\delta) = \frac{x\delta}{2300} \quad (20)$$

n is the coefficient calculated as (21).

$$n = \left|\frac{\delta_{B-(B+R)}}{\delta_{B-R}}\right| \quad (21)$$

Where $|\delta_{B\text{-}R}|$ presents the difference in vertical displacement between the nail joints in lumbers caused by only bending deformation and those caused by only rotational deformation with the support point serving as the center of rotation for the lumber. Additionally, $|\delta_{B\text{-}(B+R)}|$ represents the difference in vertical displacement between the nail joints in lumbers caused by only bending deformation and those caused by both bending deformation and rotational deformation with the support points serving as the center of rotation for the lumber.

When n is 1, the lumber with butt joints between the load points has no bending deformation but only rotational deformation with the support points serving as the center of rotation. When n is 0, the lumber with butt joints between the load points has no rotational deformation with the support points serving as the center of rotation but only bending deformation. Therefore, as n increases, the ratio of vertical displacement caused by rotational deformation out of that caused by both bending and rotational deformation in lumbers with butt joints between the load points increases, and the shear deformation of nail joints also increases.

When the displacement at the center of the span changes from δ to $\delta+\Delta\delta$, the internal energy consumption ($E_{INT\text{-}nail}(\delta \rightarrow \delta+\Delta\delta)$) caused by the shear deformation of all nail joints can be calculated as (22). The calculation is multiplied by 2 to account for two rows of nails.

$$E_{INT\text{-}nail}(\delta \rightarrow \delta+\Delta\delta) = \sum_{i=1}^{60} 2\frac{1}{2}K\{\delta_{nail(x)}(\delta)+\delta_{nail(x)}(\delta+\Delta\delta)\} \cdot \delta_{nail(x)}(\Delta\delta) \quad (22)$$

Where K represents the initial stiffness perpendicular to the grain of the nail joint (see Table 2), i is the real number representing the position along the NLT panel from the support point to the other one, and x=100i.

The total internal energy consumption is equal to the external energy consumption as given in (23), and the load required at the load points to give a specific deformation at the center of the NLT panel can be calculated.

$$\begin{aligned}E_{EXT}(\delta \rightarrow \delta+\Delta\delta) = E_{INT\text{-}beam}(\delta \rightarrow \delta+\Delta\delta) \\ + E_{INT\text{-}nail}(\delta \rightarrow \delta+\Delta\delta)\end{aligned} \quad (23)$$

By conducting an incremental displacement analysis, the load-deformation curve of the NLT panels was estimated.

Results of calculation

The results of the calculation are presented in Figure 17 as (a) NLT with the steel nail and (b) NLT with the aluminum nail, compared with the test results. The red load-deformation curves in Figure 17 represent the test results, while the black dashed lines represent the load-deformation curves obtained using the calculation method described above. These black dashed lines represent

https://doi.org/10.52202/080513-0273

several load-deformation curves with varying coefficient *n*.

The coefficient *n* that best matched the test results was approximately 0.035 for steel nails and 0.040 for aluminum nails. As n increases, the ratio of vertical displacement caused by rotational deformation to the total vertical displacement (caused by both bending and rotational deformation) in lumbers with butt joints between the load points increases. This contributes to an increase in the shear deformation of nail joints. The coefficient *n* for aluminum nails was 1.15 times that of steel nails, and the shear deformation of aluminum nails was larger than that of steel nails. In addition, the initial stiffness of the steel nails was 3.72kN/mm, while that of aluminum nails was 2.57kN/mm (see Table 2). The initial stiffness of aluminum nails was almost 70% of that of steel nails. Therefore, the ratio of vertical displacement caused by rotational deformation in lumbers with butt joints between the load points to the total vertical displacement (caused by both bending and rotational deformation) is higher with lower initial stiffness, such as aluminum nails.

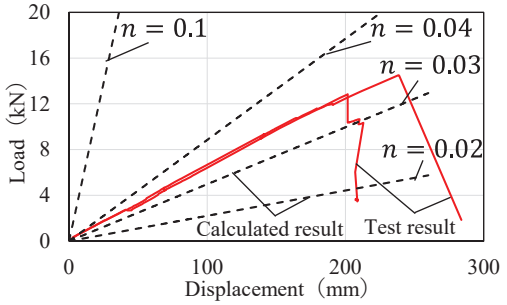

(a) steel nail

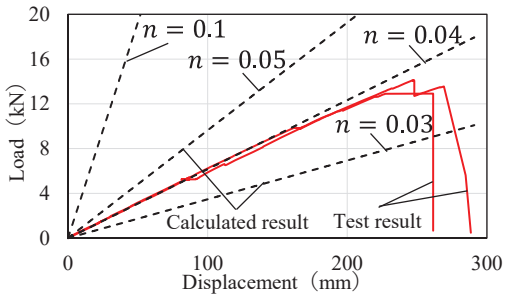

(b) Aluminum nail

***Figure 17**: Load-deformation curves, comparison of experimental and calculated results*

5 CONCLUSION

The following findings were obtained.

1 For the in-plane shear test, the initial stiffness of NLT with aluminum nails was 63% of that with steel nails. The in-plane shear capacity of NLT composed of aluminum nails was 65% of that composed of steel nails.

2 NLT with steel nails in comparison to the NLT with aluminum nails showed a higher rate of embedment workagainst the total work.

3 The bending modulus of elasticity and strength of NLTs composed of aluminum nails were almost equivalent to those composed of steel nails.

4 Lumbers joined with aluminum nails had a higher rate of rotational deformation out of the total rotational (bending and rotational deformation) compared to those joined with steel nails.

ACKNOWLEDGMENT

This research was supported by the Tochigi Prefecture Forest Research Center.

REFERENCES

[1] Nail Laminated Timber Canadian Design & Construction Guide Vol.1: Forest Innovation Investment L.t.d, 2017.

[2] Nail Laminated Timber U.S. Design & Construction Guide v1.0: Binational Softwood Lumber Council, 2017.

https://doi.org/10.52202/080513-0273